



Contents lists available at ScienceDirect

Journal of Catalysis

journal homepage: www.elsevier.com/locate/jcat

Formation of defect site on ZIF-7 and its effect on the methoxycarbonylation of aniline with dimethyl carbonate

Deliana Dahnum^{a,b}, Bora Seo^a, Seok-Hyeon Cheong^{a,b}, Ung Lee^{a,b}, Jeong-Myeong Ha^{a,b}, Hyunjoon Lee^{a,b,*}

^a Clean Energy Research Center, Korea Institute of Science and Technology, 5, Hwarang-ro 14-gil, Seongbuk-gu, Seoul 02792, Republic of Korea

^b Division of Energy & Environment Technology, KIST School, Korea University of Science and Technology, Seoul 02792, Republic of Korea

ARTICLE INFO

Article history:

Received 20 August 2019

Revised 24 September 2019

Accepted 25 September 2019

Available online xxx

Keywords:

ZIF-7

Defect site

Methoxycarbonylation

Aniline

DMC

Aromatic carbamate

ABSTRACT

The Zeolitic Imidazole Framework ZIF-7, $(\text{Zn}(\text{benzimidazole})_2)$, is known to exhibit a unique gate-opening property depending on the temperature and pressure in the presence of guest molecules, making it useful for H_2 , CO_2 , and paraffin separation technology. Besides this distinctive gas adsorption property, ZIF-7 can be used as a catalyst because it contains a Lewis acid site on Zn, and a Lewis basic site on the benzimidazole. In this study, for the first time, we demonstrate that ZIF-7 is a very promising material as a catalyst for the methoxycarbonylation of aniline with dimethyl carbonate (DMC) to produce methyl phenyl carbamate (MPC), an isocyanate precursor. Fresh ZIF-7 showed a high aniline conversion of over 95% at 190 °C for 2 h, and the yield MPC was 60–70% due to the formation of methylated side products, such as *N*-methyl aniline and *N,N*-dimethylaniline. However, interestingly, when the ZIF-7 was reused, the yield of MPC gradually increased and reached over 94.7% by the catalyst's 6th run. SEM and TEM images revealed the crystalline structure of ZIF-7 collapsed during the reaction due to the leaching of benzimidazole from the ZIF-7, which created defect sites on the Lewis acidic zinc center. Based on ^1H NMR and XPS studies, it can be assumed that the DMC binds to the Zn defect sites on the ZIF-7, activating the carbonyl groups on DMC, resulting in the increased selectivity to methoxycarbonylation compared to methylation. Pretreating ZIF-7 with DMC at 190 °C for 6 h could directly activate the ZIF-7 for this methoxycarbonylation reaction. The activated ZIF-7 showed 91.0% MPC yield and the catalyst was reusable.

© 2019 Elsevier Inc. All rights reserved.

1. Introduction

Carbamate is one of the attractive green chemicals that can avoid toxic phosgene during the production of isocyanate. One of the issues in the development of catalysts for the methoxycarbonylation of aromatic amine with DMC is related to their selectivity to the product. As can be seen in Scheme 1, DMC can act as a methylating agent as well as methoxycarbonylation agent [1,2]. One way of increasing the selectivity to the methoxycarbonylation reaction is to use a Lewis acid as a catalyst, which activates the carbonyl groups on the DMC, thereby facilitating the nucleophilic attack of amine. Accordingly, many Lewis acid catalytic systems have been reported, including metal salts based on zinc [3,4], lead [5,6] and ytterbium [7]. Among these catalysts, homogeneous zinc acetate

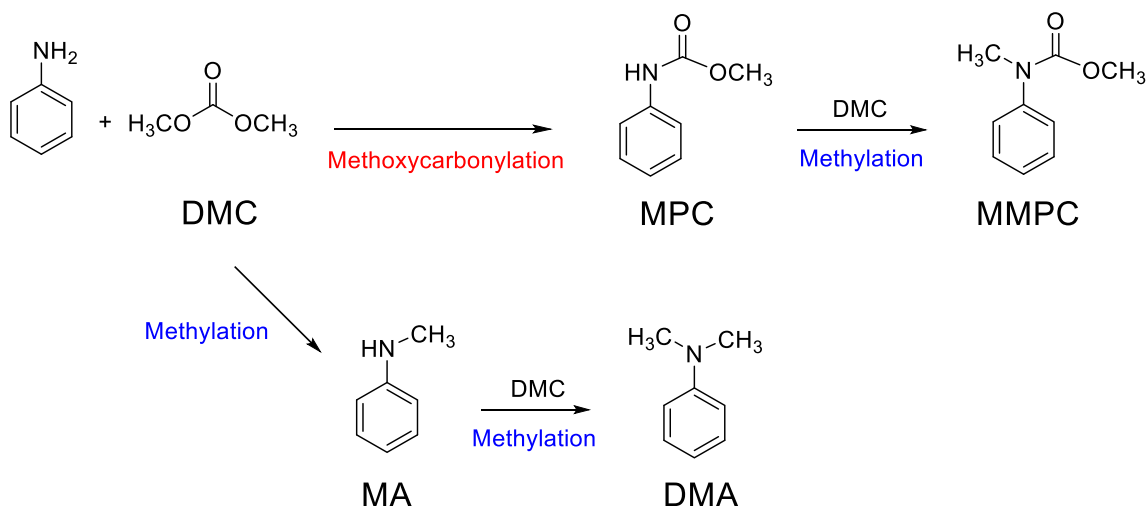
is known to be the best catalyst, however, during the reaction, zinc acetate turns into ZnO and loses its activity [6].

To overcome the limitations of a homogeneous catalyst system, which include difficulties with catalyst separation from the product mixture and recycling after the reaction, immobilizing of Zn $(\text{OAc})_2$ on a solid support has been investigated. Zhao et al. showed that Zn $(\text{OAc})_2$ supported on activated carbon produced MPC with a yield of 78% and a selectivity of 98%; however, serious leaching of the active component was observed [8]. Li et al. also anchored Zn $(\text{OAc})_2$ onto the surface of SiO_2 and found that a high MPC yield of 93.8% could be achieved, but the catalytic activity decreased during reuse due to the formation of zinc oxide [9]. Deactivation of the catalyst due to decreased support area also occurred when ZnO-TiO₂ and ZrO₂-SiO₂ were used in the reaction [10,11]. The mesoporous catalyst AlSBA-15 showed recyclability after calcination at 550 °C in air and yielded 70.3% of MPC [12].

On the other hand, Guo et al. immobilized zinc ions on SBA-15 which contain carboxylate functional groups [13]. Using the synthesized heterogeneous catalyst, the methoxycarbonylation of 4,4'-methylenedianiline (MDA) with dimethyl carbonate was

* Corresponding author at: Clean Energy Research Center, Korea Institute of Science and Technology, 39-1 Hawolgok-dong, Seongbuk-gu, Seoul 02792, Republic of Korea.

E-mail address: hjlee@kist.re.kr (H. Lee).



Scheme 1. Reaction of aniline with dimethyl carbonate (DMC). MPC: methyl phenyl carbamate, MMPC: methyl *N*-methyl-*N*-phenyl carbamate, MA: *N*-methylaniline, DMA: *N,N*-dimethylaniline.

effectively achieved, although catalyst deactivation was observed during reuse. Similarly, Wang et al. also synthesized zinc alkyl carboxylate which was chemically bonded onto a silica surface [14]. It was found to possess a cyclic single catalytic site which was highly active and recyclable. Although both catalyst systems had catalytic activity comparable to homogeneous $\text{Zn}(\text{OAc})_2$, their complicated synthesis processes could be an obstacle to the practical application of the catalysts.

Zeolitic Imidazole Frameworks (ZIFs), ZIFs, a subclass of metal-organic frameworks (MOFs), are attracting great attention due to their large surface area, facile synthesis as well as high chemical and thermal stabilities [15,16]. Accordingly, this material has great applications as sensors for chemical compounds, membrane separation, and adsorbents for hydrogen, methane, ethane, and CO_2 gas [17–24]. Furthermore, besides acting as a catalyst support for metal nanoparticles or transition metal complexes, ZIF itself has shown good catalytic activities for the Knoevenagel reaction [25], the coupling reaction of epoxide and CO_2 [26,27], olefin epoxidation [28], esterification [29], transesterification [30], and etc.

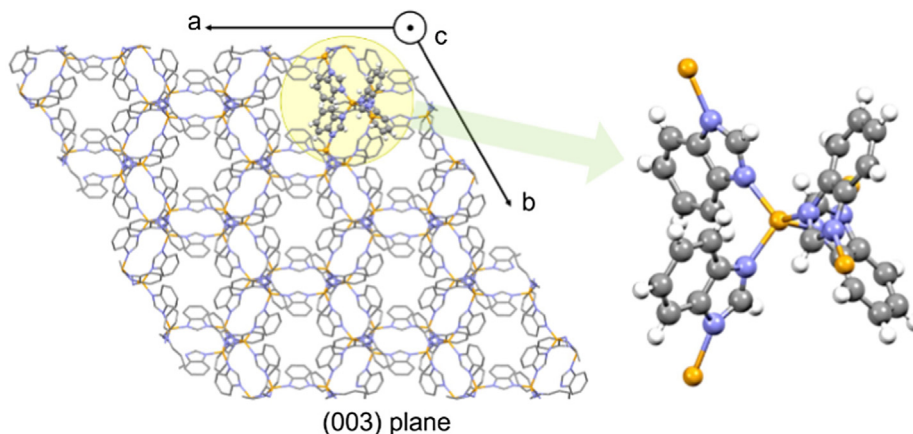
ZIF-7 composed of Zn metal connected with a 1H-benzimidazole linker is a typical ZIF with sodalite (SOD) framework topology (Scheme 2). Interestingly, it has a very distinctive property, the gate opening effect [31]. It was reported that, due to the flexible benzimidazole linker, a non-destructive structural

change from narrow pore phase to large pore phase can occur depending on the temperature and pressure in the presence of guest molecules like CH_4 , CO_2 and light olefins [32]. Many structural investigations have been conducted to understand this gate opening phenomenon, and it has been employed for the separation of paraffin/olefin, water/ethanol, CH_4 and CO_2 from N_2 .

Like other ZIF materials, ZIF-7 has a Lewis acidic site and basic site on the zinc metal and benzimidazole, respectively. This means it should be able to act as a catalyst for both Lewis acid or Lewis base-catalyzed reactions. However, to the best of our knowledge, the catalytic activity of ZIF-7 has not been studied in any catalytic reactions.

In this study, we used ZIF-7 as a catalyst for the methoxycarbonylation of aniline and found that defects were formed on the ZIF-7 during the reaction. The ZIF-7 with defect sites showed enhanced catalytic performance for the methoxycarbonylation reaction compared to the fresh ZIF-7.

Frequently, the defect sites on MOFs or ZIFs have played a critical role in some catalytic reactions [33]. Vermoortele et al. reported the catalytic activity of zirconium terephthalate UiO-66 (Zr) could be increased by treating the catalyst with trifluoroacetic acid which affects the formation of the open metal site [34]. Chizallet et al. supposed that the high activity of ZIF-8 for transesterification may come from the strong Lewis acid sites of $\text{Zn}(\text{II})$, and



Scheme 2. Structure of ZIF-7. Zn, yellow; N, blue; C, gray; H, white.

Bronsted acid sites (NH group) [30]. Meanwhile, Tian et al. and Lee et al. showed the surface of ZIF-8 was covered with various groups such as carbonate, water/hydroxide, and secondary amines in the surface of the material, which affected the separation ability of ZIF-8 [35,36].

We analyzed the used catalyst by SEM, ^1H NMR, XPS, and XANES and proved that benzimidazole was leached from the Zn center during the reaction, forming a catalytic active site on the surface of the ZIF-7. Based on this observation, we proposed a catalytic mechanism for this reaction.

2. Experimental section

2.1. General

All chemicals used in this study were of analytical grade, commercially available, and were used without further purification. Zinc acetate dihydrate and methyl phenyl carbamate were purchased from Kanto and Tokyo Chemical Industries (TCI) Co. Ltd, respectively. The other chemicals were purchased from Sigma-Aldrich.

2.2. Catalyst preparation

A series of ZIF-7 was synthesized according to the reported method [37]. Zinc precursor, including $\text{Zn}(\text{OAc})_2$, ZnCl_2 , and ZnBr_2 , benzimidazole, and diethylamine in DMF were heated in the bomb reactor system with stirring at 130°C for 48 h, while $\text{Zn}(\text{NO}_3)_2$ was reacted at RT. After the reaction, the formed solid was filtered and washed with DMF three times. The isolated solid was dried at 160°C for 3 h under vacuum to remove DMF. The synthesized material was stored in the glove box before use. Detailed syntheses methods and XRD analyses results of produced ZIF-7 according to the used zinc precursor were described in Supporting Information and Fig. S1.

2.3. Methoxycarbonylation

Catalytic reaction was conducted in a high-pressure Parr reactor (100 mL) equipped with glass liner and a magnetic-driven mechanical stirrer. 12.5 mmol (1.16 g) of aniline and 150 mmol (13.5 g) of DMC were added in glass liner together with 0.116 g (10 wt%) of catalyst and 0.5 g of toluene as an internal standard. After purging the reactor with N_2 (>99.9%) twice, the temperature was increased to 190°C with a $4^\circ\text{C}/\text{min}$. After 2 h, the reactor was cooled to room temperature. Quantitative analysis of product in solution was performed by using Gas Chromatography (Aligent 7890A) with an HP-5 capillary column ($30\text{ m} \times 0.32\text{ mm} \times 0.25\text{ }\mu\text{m}$) and a FID detector. Typical GC-chromatogram was shown in Fig. S2 in Supporting Information.

The conversion of aniline, yields of products including MPC, MMPC, MA, and DMA were calculated as following equations. Three kinds of ureas, diphenyl urea, N-methyl-diphenyl urea, and N,N'-dimethyl-diphenyl urea, were produced together with a minor concentration. The total yield of ureas was measured by subtracting the yields of MPC, MMPC, MA, and DMA from the conversion of aniline.

$$\text{Conv. of aniline}(\%) = \frac{\text{Initial aniline (mmol)} - \text{Unreacted aniline (mmol)}}{\text{Initial aniline (mmol)}} \times 100\%$$

$$\text{Yield of product}(\%) = \frac{\text{Product (mmol)}}{\text{Initial aniline (mmol)}} \times 100\%$$

$$\text{Yield of ureas}(\%) = \text{Conv. of aniline}(\%)$$

$$- \text{Yield of products (MPC + MMPC + MA + DMA)}(\%)$$

For the reuse of the catalyst, after the reaction, the catalyst was separated from the reaction mixture by centrifugation. A spent catalyst was washed with DMC and dried at 60°C for 3 h under vacuum.

2.4. Characterization of catalyst

The XRD pattern of ZIF-7 before and after the reaction was obtained by Shimadzu X-ray diffractometer (XRD-6000, Japan) using nickel-filtered $\text{CuK}\alpha$ radiation with the 2θ angle between 5° and 80° . GC-MS (HP- 6890 GC with a 5973 Mass spectrometer) was used to confirm the products. Zinc concentration was measured by ICP-AES (Thermo scientific iCAP 7000). Proton NMR was carried out on a Bruker Avance 400 MHz (Bruker Corp.: Billerica, MS, USA). For the preparation ^1H NMR samples, 0.05 g of ZIF-7 was diluted in 0.5 g D_2SO_4 and 0.5 g H_2SO_4 including 10 wt% of methanesulfonic acid as an internal standard. Scanning Electron Microscopy (SEM) of samples was accomplished using a field-emission scanning electron microscope (FEI Inc., NovaNano 200, Hillsboro and Teneo VS). CHN analysis was conducted using Thermo scientific Flash 2000. Transmission electron microscopy (TEM) images were taken by FEI Tecnai F20 G2 at an acceleration voltage of 200 kV. XAS was performed at the beamline 8C of the Pohang Accelerator Laboratory (PAL). The incident X-ray had the electron beam energy and current of 3.0 GeV and 300 mA, respectively. A Si (1 1 1) double crystal monochromator was used to filter the incident photon energy, which was detuned by 30% to remove high-order harmonics.

3. Results and discussion

3.1. Methoxycarbonylation using ZIF-7

Four kinds of zeolitic imidazole framework-7 (ZIF-7) complexes were synthesized by the reaction of zinc compounds of $\text{Zn}(\text{OAc})_2$, ZnCl_2 , ZnBr_2 , and $\text{Zn}(\text{NO}_3)_2$ with benzimidazole, using DMF as the solvent as described in the experimental part. The resulting materials were designated ZIF-7-OAc, ZIF-7-Cl, ZIF-7-Br, and ZIF-7- NO_3 according to the zinc precursors used. After synthesis, all products were activated at 160°C for 3 h under vacuum to remove the solvent.

CHNZn analyses results shown in the Supporting Information reveal the empirical formula of ZIF-7 from ZnCl_2 , ZnBr_2 , and $\text{Zn}(\text{NO}_3)_2$ were very close to $\text{Zn}(\text{Belm})_2$, however, the shapes and surface areas were different according to the zinc precursor used [37]. Fig. 1 and Table S1 show that ZIF-7-OAc has a rhombic-dodecahedral shape with a BET surface area of $75\text{ m}^2\text{ g}^{-1}$, while ZIF-7-Cl and ZIF-7-Br had a rod morphology with BET areas of 12 and $19\text{ m}^2\text{ g}^{-1}$, respectively. ZIF-7- NO_3 showed the highest surface area of $110\text{ m}^2\text{ g}^{-1}$ which originated from its small spherical particles and amorphous nature, as shown in Fig. 1. We expected that those different morphologies and surface areas could result in different catalytic activities during the methoxycarbonylation reaction, but they showed very similar results.

Fig. 2 revealed when the synthesized ZIF-7s were used as a catalyst for the methoxycarbonylation of aniline with dimethyl carbonate (DMC) at 190°C for 2 h, the aniline was converted almost quantitatively in all the reactions. They produced methyl phenyl carbamate (MPC) with similar yields between 61.9 and 70.7%. Contrary to our expectation, ZIF-7- NO_3 which had the highest surface area exhibited the lowest MPC yield of 61.9%. As described in the

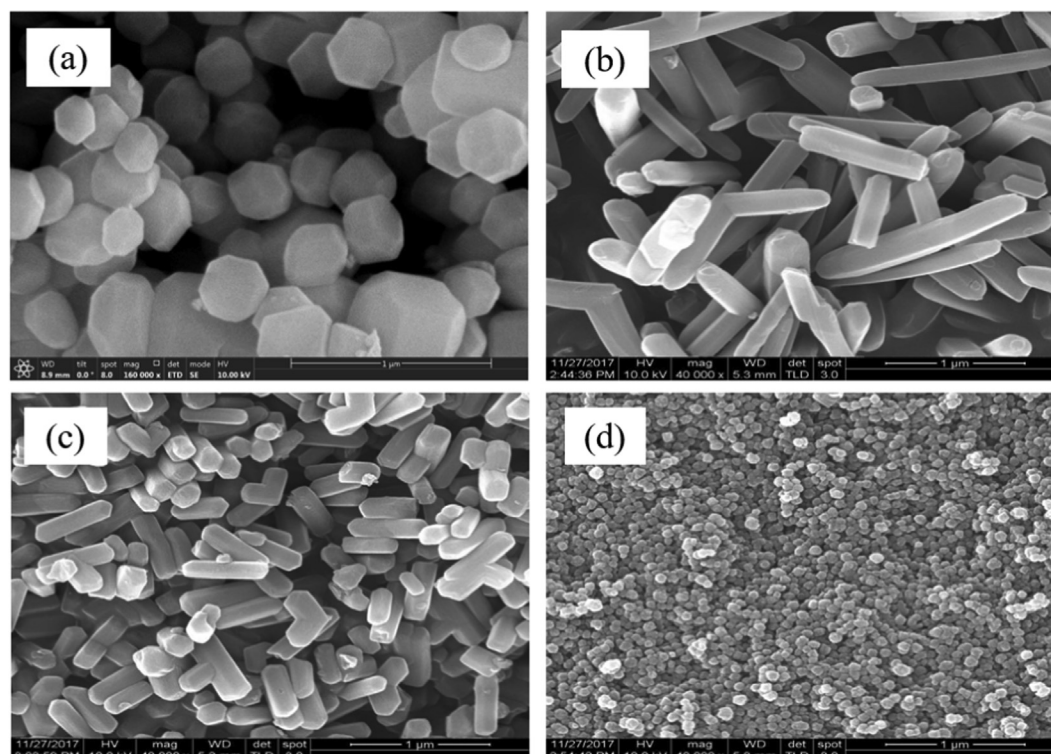


Fig. 1. SEM images of various ZIF-7 synthesized from (a) $\text{Zn}(\text{OAc})_2$, (b) ZnCl_2 , (c) ZnBr_2 , (d) $\text{Zn}(\text{NO}_3)_2$.

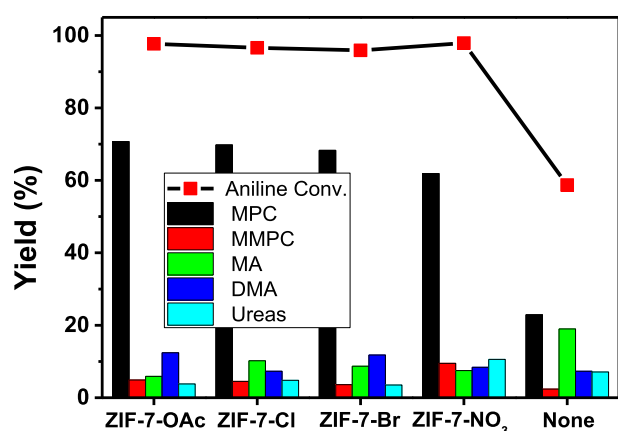


Fig. 2. Methoxycarbonylation of aniline with DMC using various ZIF-7s. Reaction condition: aniline 1.16 g, DMC 13.5 g, catalyst 0.116 g, 190 °C, 2 h.

introduction section, DMC also acted as a methylating agent to produce methylated MPC (MMPC), N-methylaniline (MA) and N,N-dimethylaniline (DMA). They were formed with yields between 4.5 and 12.4%. Diphenyl urea and its methylated derivatives made from MPC and aniline were also detected. In the absence of a catalyst, aniline conversion was 55% and MPC yield was 22.9%. The formation of methylated side products, MA and DMA, were slightly higher than those of the ZIF-7-catalyzed reaction. They were 13.0% and 14.6% yields for MA and DMA, respectively.

On the other hand, as S. Grego et al proposed, the formation of MMPC and DMA seems to be formed via MPC and MA, respectively, as shown in Scheme 1 [38]. The effect of reaction time on the selectivities of MPC, MMPC, MA, and DMA support this assumption (Fig. S3). For the ZIF-7-catalyzed reaction shown in Fig. S3(a), MPC selectivity reached its maximum after 2 h reaction, and decreased at 4 h with an increase in MMPC. In the case of MA, it

showed the highest selectivity at 30 min reaction, and decreased after that, while, DMA selectivity increased constantly with the reaction time. In the catalyst-free reaction, although the conversion of aniline and selectivity to MPC were much lower than in the ZIF-7-catalyzed reaction, similar selectivity changes between MPC-MMPC and MA-MMA were observed according to reaction time (Fig. S3(b)).

Over all, these results indicate ZIF-7 promoted methoxycarbonylation rather than methylation, but its yield and selectivity to MPC were poorer compared to the homogeneous catalyst system, which reduces the advantages of the heterogeneous catalyst. However, interestingly, when the catalyst was reused, the yield and selectivity to MPC increased significantly.

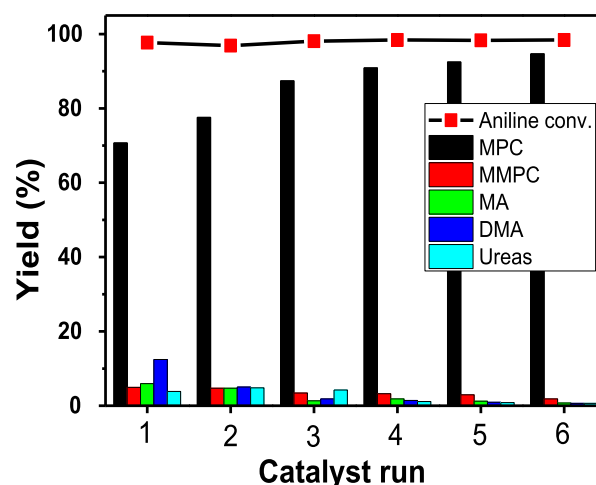


Fig. 3. Reuse of ZIF-7 for the methoxycarbonylation of aniline with DMC. Reaction condition: aniline 1.16 g, DMC 13.5 g, catalyst 0.116 g, 190 °C, 2 h.

3.2. Catalyst reuse

For the catalyst reuse experiment, ZIF-7 synthesized from Zn(OAc)₂ was used. After the 1st reaction, the catalyst was filtered out, washed with DMC, and dried at RT under vacuum for 3 h and then used again. Fig. 3 show that with increasing catalyst reuse, the yields of MPC increased. When the ZIF-7 isolated from the 1st reaction was used again, the yield of MPC increased to 77.6% from 70.7%. Furthermore, the MPC yield increased further and reached 94.7% by the 6th run. This MPC yield is similar to those from homogeneous Zn, Pb, and Yb-based methoxycarbonylation reaction and belongs to one of the highest MPC yield reported at the heterogeneous catalyst reaction (Table 1). Whereas, the yields of methylated products decreased by a substantial degree with the catalyst reuse. The formation of MA and DMA, which were 5.9 and 12.4% in the first reaction, were reduced to 0.7 and 0.6% in the 6th

run, respectively. The same phenomena were observed with the other ZIF-7s prepared from ZnCl₂, ZnBr₂, and Zn(NO₃)₂ (Fig. S4).

3.3. Characterization of the used ZIF-7

The increased selectivity to MPC with catalyst reuse indicates that some properties of the ZIF-7 changed during the reaction. To elucidate the reason for the increased catalytic activity, the morphologies of the catalyst before and after the reaction were observed using SEM and TEM. Fig. 4 and Fig. S5 show, fresh ZIF-7 made from Zn(OAc)₂ had a very regular rhombic-dodecahedral structure. However, after the reaction, the crystal structure of ZIF-7 was destroyed. The structures were worn and broken, and the surface of the ZIF-7 was rough and had cracks. In addition, some particles appeared to be agglomerated. As the number of uses increased, the degree of structural changes increased.

Table 1

Comparison of catalytic activities of various catalysts at the methoxycarbonylation of aniline or its derivatives with DMC

Entry.	Catalyst	Reaction Condition (Temp., reaction time, catalyst amount)	Carbamate Yield (%)	Remarks	Ref.
Homogeneous					
1	Zn(OAc) ₂ ·2H ₂ O	120 °C, 190 min, 4 mol%	85	Deactivation to ZnO	3
2	Zn ₄ O(O ₂ CCH ₃) ₆	180 °C, 2 h, 0.25 mol%	96	–	4
3	PbO	160 °C, 1 h, 12 mol%	96.7	–	5
4	Pb(OAc) ₂	170 °C, 4 h, 2 mol%,	97.7	Deactivation to Pb ₃ (CO ₃) ₂ (OH) ₂	6
5	Yb(OTf) ₃	80 °C, 8 h, 5 mol%	96	Extraction of catalyst using CH ₂ Cl ₂	7
Heterogeneous					
6	ZIF-7 (DMC-treated)	190 °C, 2 h, 10 wt%	91.0	Reusable	This work
7	Zn(OAc) ₂ /AC	150 °C, 4 h	78.0	Leaching of Zn(OAc) ₂	8
8	Zn(OAc) ₂ /SiO ₂	170 °C, 7 h, 30 wt%	93.8	Deactivation to ZnO	9
9	ZnO-TiO ₂	170 °C, 7 h, 25 wt%	66.7	Deactivation	10
10	ZrO ₂ /SiO ₂	170 °C, 7 h, 25 wt%	79.8	Deactivation	11
11	Al/SBA-15	100 °C, 3 h, 53 wt%	71.0	Reusable after calcination	12
12	Zinc carboxylate/SBA-15 ^c	170 °C, 4 h, 20 wt%	86.5	Slight deactivation with reuse	13
13	Zinc alkyl carboxylate on silica	170 °C, 2 h, 0.5 mol% Zn	91.6	Reusable	14

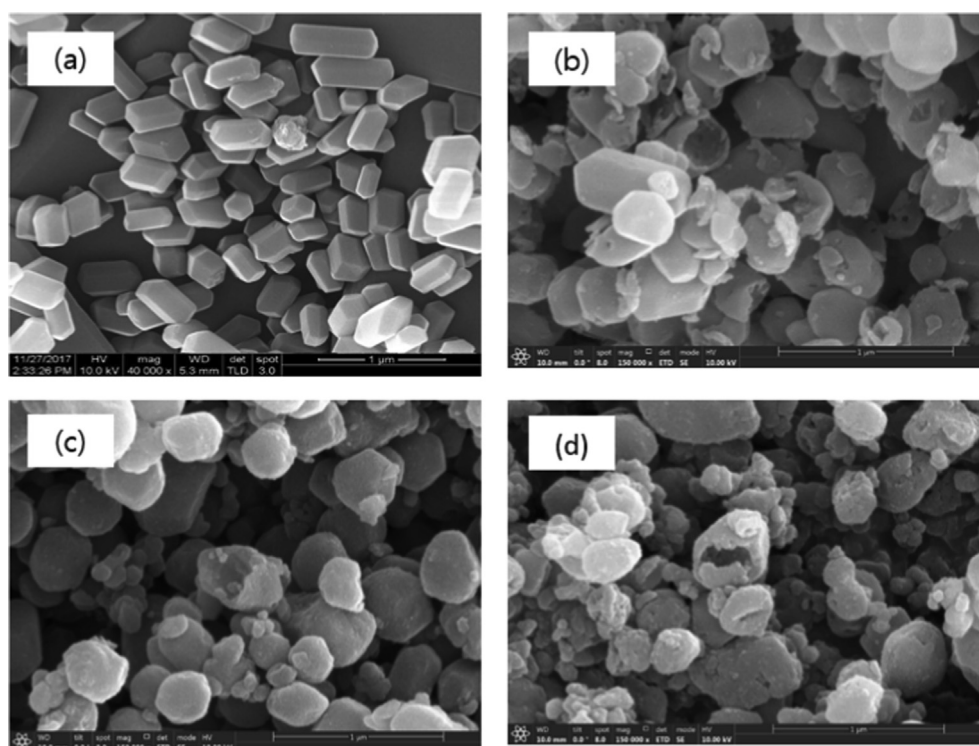


Fig. 4. SEM images of ZIF-7 made from Zn(OAc)₂ (a) fresh, (b) after 2nd run, (c) after 4th run, and (d) after 6th run.

XRD spectra, which are shown in Fig. 5, also gave similar results. The intensities of the characteristic peaks of ZIF-7 at 13.3° , 15.4° , 16.2° , and 19.8° which correspond to the (0 3 0), (2 2 0), (-1 3 2), and (3 1 2) planes [15], decreased with increasing catalyst reuse, confirming the destruction of the crystalline phase in ZIF-7 after the reaction. However, interestingly, the intensity of the peak at 7.7° , which is the (1 1 0) plane, increased with reuse.

Previously, ZIFs like ZIF-7 and ZIF-8 have been known to have a reversible structural change called ‘gate opening’ or ‘breathing’ under CO_2 pressure, C2-C3 alkane adsorption, or solvent substitution [23,24,39,40]. During the structural changes, the pores in ZIF-7 transform from a narrow pore phase (np-phase) to a large pore phase (lp-phase), which can be distinguished in the XRD peaks, at 8.6° and 9.5° for the np-phase and 7.7° for the lp-phase. In our study, the np-phase was also detected at 8.6° and 9.5° in the fresh ZIF-7, but they shifted slightly to 8.3° and 9.2° after 2nd run, indicating the pores had become larger during the reaction. After the 4th run, these np peaks disappeared and the lp-phase became stronger.

The collapse of the crystal structure of the ZIF-7 during the reaction can be attributed to a change in the chemical composition of ZIF-7 by the leaching of the ligand, benzimidazole, and/or zinc component. This creates a defect site on the catalyst, which can act as an active catalytic site for the methoxycarbonylation reaction.

Zhang et al. computationally examined the thermodynamic stability and kinetic accessibility of various point defects in ZIF-8, $\text{Zn}(\text{2-methylimidazolate})_2$, and found that several of the defect structures were lower in energy relative to the defect-free parent crystal [41]. They suggested three kinds of point defects; linker vacancy, zinc vacancy, and dangling linker. In this study, we deduced the formation of a linker vacancy in the ZIF-7 during the reaction, by the leaching of benzimidazole, which resulted in the exposure of a Lewis acidic zinc site in the reaction media.

The ligand change in ZIF-7 after the reaction was also observed in X-ray absorption near-edge structure (XANES) spectra. Fig. 6 shows that the edge lines of the spectra for the catalyst before and after the reactions are overlapped, indicating that the oxidation state of Zn was almost retained [42]. There was a negligible shift in the binding energies of zinc before and after the reactions. The white line peaks that appeared around 9665 eV and 9672 eV (denoted I and II, respectively) are related to the $1s \rightarrow 4s$ transition, and their intensities are affected by the coordination environment [42]. More specifically, peak I dominates when Zn is

coordinated with oxygen atoms like Zn acetate, and peak II is significant in the Zn imidazole complex, where Zn is coordinated to four N atoms [43,44]. After the 4th run, peak I increases and peak II decreases, suggesting increased Zn–O coordination and decreased Zn–N coordination, respectively.

The amount of leached benzimidazole from the catalyst and the types of attached chemical species on the vacant zinc sites could be estimated using ^1H NMR and ICP analyses. When ZIF-7 is dissolved in D_2SO_4 , it is destructed to zinc ion and benzimidazole, which enable the quantification of the zinc and benzimidazole in the ZIF-7. As Fig. 7 and Table S2 show, in ^1H NMR the fresh ZIF-7 only had benzimidazole, and the amount of benzimidazole with respect to Zn was 2.06, which was close to the empirical formula of ZIF-7, $\text{Zn}(\text{Belm})_2$. However, after the 2nd run, the molar ratio of benzimidazole to Zn became 1.86 and it decreased further to 1.44 after the 6th run.

Interestingly, new peaks with apparent intensities were observed in the reused catalysts, whose positions overlapped the peaks of MPC and methanol. MPC and methanol species are reaction products of this methoxycarbonylation reaction. Therefore,

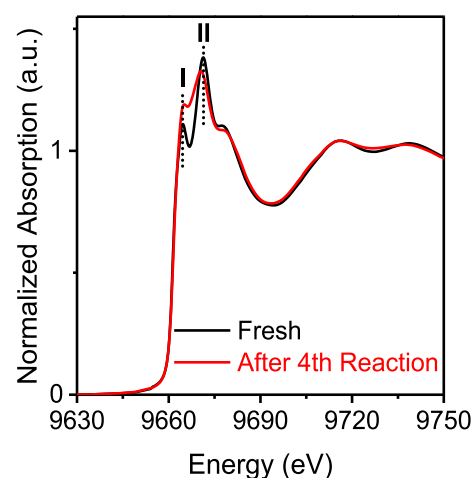


Fig. 6. X-ray Absorption Near Edge Spectra (XANES) of ZIF-7.

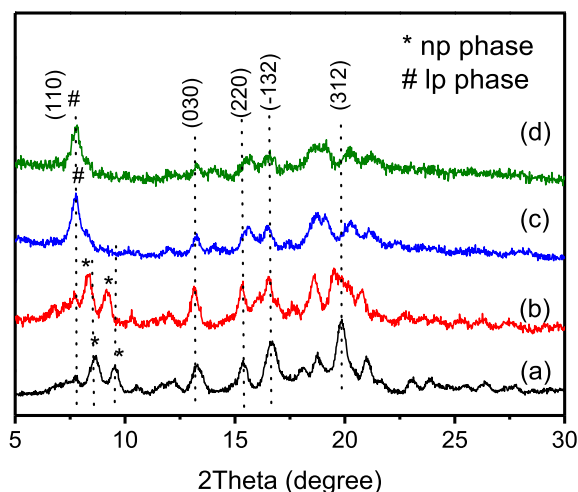


Fig. 5. XRD patterns (a) fresh ZIF-7 and used ZIFs (b) after 2nd run, (c) after 4th run, and (d) after 6th run.

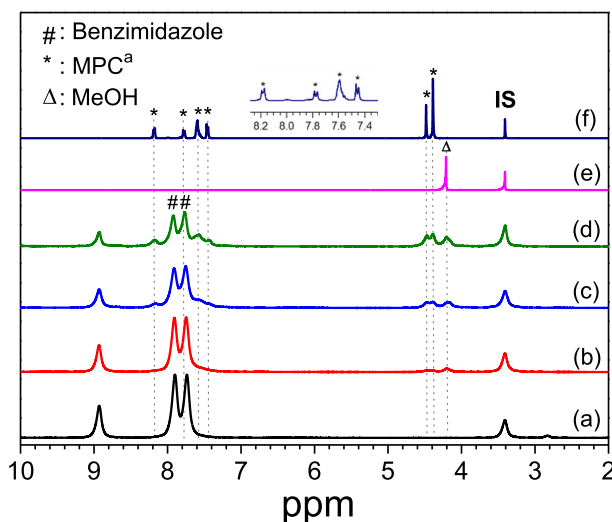


Fig. 7. ^1H NMR spectra of (a) fresh ZIF-7, (b) ZIF-7 after 2nd run, (c) ZIF-7 after 4th run, (d) ZIF-7 after 6th run, (e) MeOH, (f) MPC. All NMR spectra were measured in D_2SO_4 . ^a Detailed explanation about the ^1H NMR of MPC was described in Supporting information.

they could occupy the vacant sites in Zn formed by the leaching of benzimidazole.

These results indicate MPC and/or methanol might be the species that facilitate the leaching of benzimidazole, thereby enhancing the yield of MPC on ZIF-7. However, a pretreatment study revealed the critical species in the activation of ZIF-7 was DMC, instead of MPC and methanol.

3.4. Pretreatment of ZIF-7 with DMC

When ZIF-7 was pretreated with DMC, aniline, MPC, and methanol at 190 °C for 6 h, respectively, and used as a catalyst, only the catalyst treated with DMC showed an increased MPC yield of 91.0% with decreased methylated product formation comparable to the value of ZIF-7 at the 4th run (Fig. 8). Meanwhile, the aniline, MPC, and MeOH didn't show any positive effect on the MPC yields and methylation products. This result indicates the DMC plays a critical role in the activation of ZIF-7 for this reaction. Furthermore, ^1H NMR analysis of the DMC-treated ZIF-7 showed a peak at 4.19

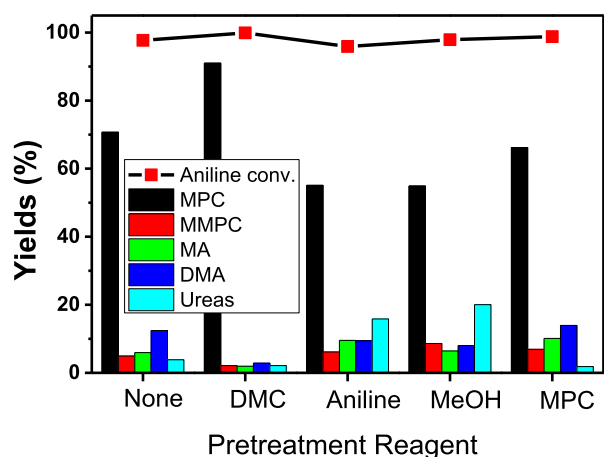


Fig. 8. Effect of treatment reagent on the methoxycarbonylation reaction. Pretreatment condition: 190 °C, 6 h. Reaction condition: aniline 1.16 g, DMC 13.5 g, catalyst 0.116 g, 190 °C, 2 h.

ppm, a methanol peak, while no peak was detected for the MeOH-treated catalyst (Fig. S7).

Therefore, it is reasonable to assume that the detected methanol species in the ^1H NMR spectrum of the used catalyst originate from the DMC, which occupies a position of the leached benzimidazole. The reaction between DMC and ZIF-7 seems to be caused by the small amount of water contained in the DMC, as described in the first reaction in Scheme 3. Formed Zn-OH can react with DMC to produce Zn-OCO₂CH₃ with the liberation of methanol. In the presence of D₂SO₄ for ^1H NMR measurement, it could be destructed to methanol and CO₂.

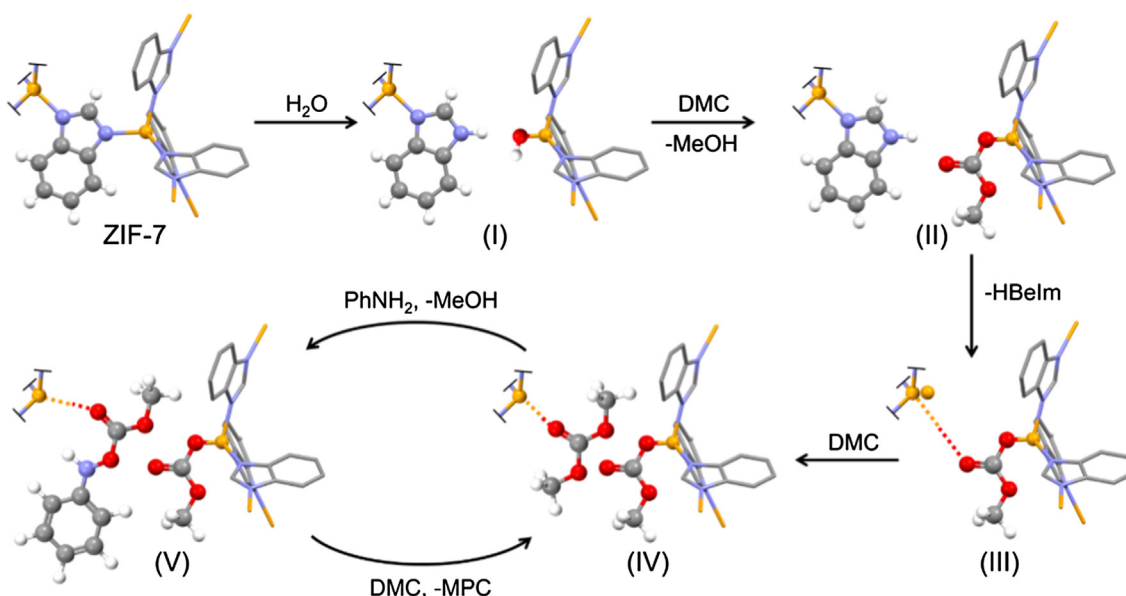
The XPS analyses shown in Fig. 9 also supports the presence of carbonyl groups on the ZIF-7 after the DMC treatment. After the 4th run, a new peak at the 289.0 eV was detected in the C1s XPS spectrum, which correspond to O-(C=O)-O. Similarly, when ZIF-7 was treated with DMC for 6 h, the same carbonate peak was observed, suggesting the carbonate group was attached to the ZIF-7 by the treatment with DMC.

Although we couldn't observe any deactivation tendency with catalyst reuse, as shown in Fig. 3, the continuous leaching of benzimidazole by DMC from the ZIF-7 could result in the complete deconstruction of the catalyst. However, interestingly, when fresh ZIF-7 was treated with excessive DMC at 190 °C for 48 h, the molar ratio of benzimidazole to zinc was 1.48, which was a value similar to that of ZIF-7 after the 6th run.

On the other hand, the formation of methylated side product seems due to the dissociated benzimidazole in the solution. When the reaction was proceeded by adding benzimidazole, methylated products were major reaction products (Fig. S8). Therefore, it can be assumed that, with repeated catalyst use, the benzimidazole concentration in the solution decreased and the reactions happened on the Lewis acidic Zn catalytic centers. As a result, methoxycarbonylation became dominant over the methylation reaction.

3.5. Optimization of reaction condition

Based on the results mentioned earlier, when ZIF-7 is pretreated with DMC before the reaction, a higher MPC yield can be obtained from the first reaction. To determine the best pretreatment conditions, fresh ZIF-7 was pretreated with DMC at various tempera-



Scheme 3. A plausible mechanism of methoxycarbonylation reaction on ZIF-7. Zn, yellow; N, blue; C, gray; H, white; O, red.

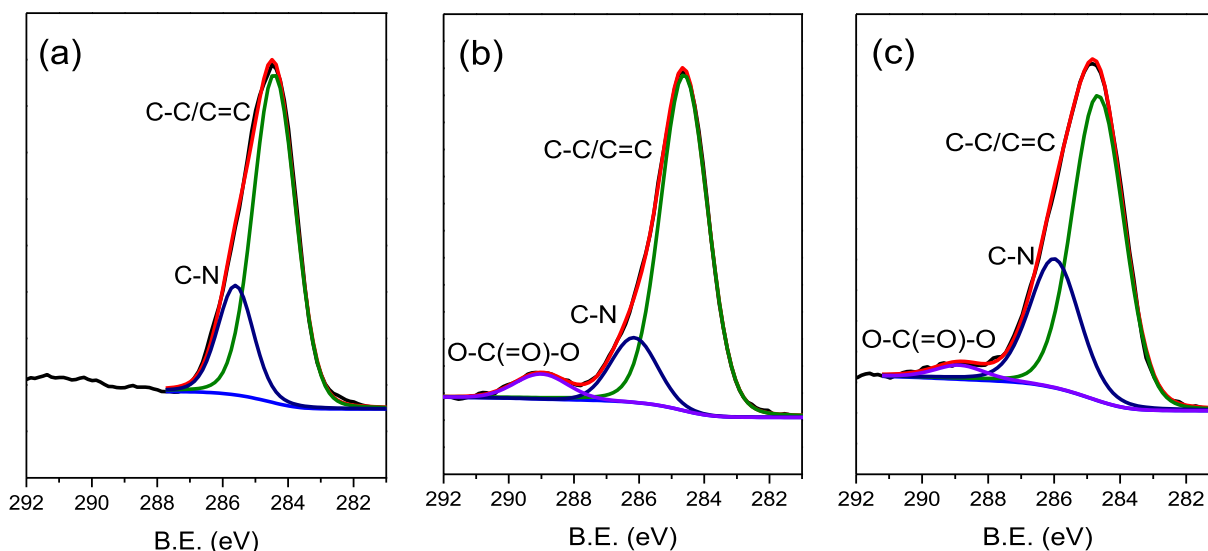


Fig. 9. XPS analyses ZIF-7 (a) fresh, (b) after 4th run, and (c) after pretreatment with DMC for 6 h at 190 °C.

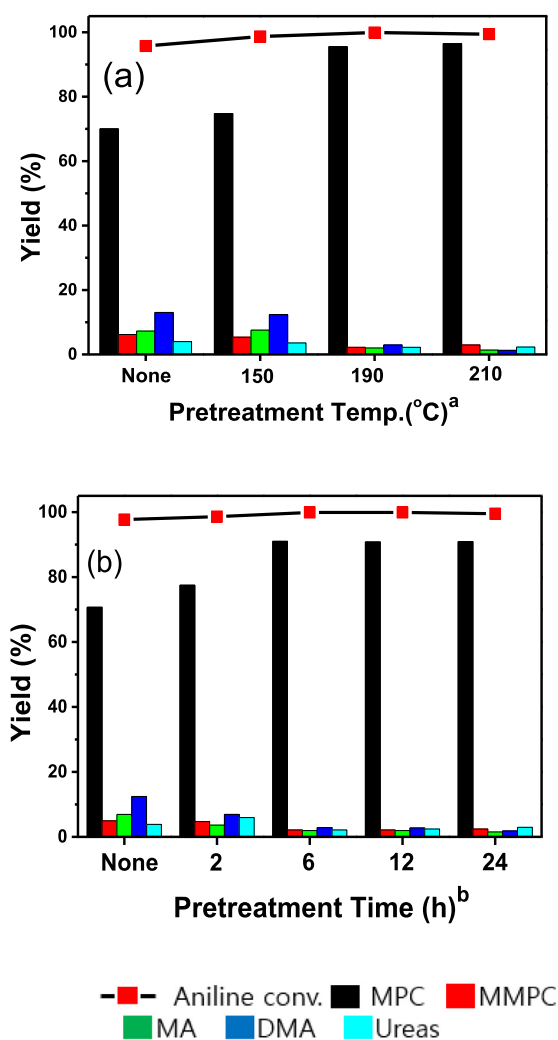


Fig. 10. Effects of (a) pretreatment temperature and (b) time using DMC on the ZIF-7-catalyzed methoxycarbonylation reaction. ^aPretreatment time was 6 h. ^bPretreatment temp. was 190 °C. Reaction condition: aniline 1.16 g, DMC 13.5 g, catalyst 0.116 g, 190 °C, 2 h.

tures and times before the methoxycarbonylation reaction. Fig. 10 shows that the optimum pretreatment temperature and time were 190 °C and 6 h; MPC yield was 91.0% which is comparable to the best heterogeneous catalyst reported (Table 4). However, when the ZIF-7 was pretreated at 150 °C for 6 h, a substantial degree of methylated side products were formed; selectivity to MPC was 72.1%. Interestingly, the MPC yield of the pretreated catalyst at 210 °C was 91.9%, which is similar to the value at 190 °C. This result suggests the DMC-treated ZIF-7 is stable at this temperature. Meanwhile, increasing in the pretreatment time to longer than 6 h didn't affect the yield of MPC.

The catalytic activities of the ZIF-7 pretreated with DMC at 190 °C for 6 h were investigated under the various reaction conditions. Fig. 11(a) shows that the MPC yield is highly dependent on the reaction temperature. At 150 and 170 °C, the conversion of aniline was 24.4 and 66.6%, respectively. Meanwhile, at the higher reaction temperature of 210 °C, the MPC yield was only 47.3% due to the formation of methylated side products. With a shorter reaction time, less than 2 h, insufficient aniline conversion was observed, less than 85%. The longer reaction time of 4 h gave increased the formation of methylated byproducts and ureas, resulting in a decreased MPC yield of 69.8% (Fig. 11(b)). The effect of the catalyst amount shown in Fig. 11(c) revealed that 10 wt% of ZIF-7 to aniline was the best ratio. At the catalyst amounts of 5 wt% and 20 wt%, the formation of side products were increased. The effect of aniline/DMC molar ratio was found to greatly affect to the reaction. As shown in Fig. S9, when the DMC/aniline molar ratio was 12 and 10, the amount of MPC and methylated side products formed were almost similar. However, at the DMC/aniline molar ratios of 8 and 5, the yield of methylated side products increased remarkably. Furthermore, increasing the aniline concentration also resulted in an increase in the urea component. Therefore, to obtain a high MPC yield, the molar ratio of DMC/aniline apparently needs to be equal to or higher than 10.

The DMC-pretreated ZIF-7 catalyst was found to be very reusable. Fig. 11(d) shows a slight increase in MPC yield to 94.7% was obtained at the 4th catalyst reuse.

3.6. Reaction mechanism

As Chizallet et al. mentioned, the first step in the dissociation of the ligand from ZIF-7 seems to start with the reaction between

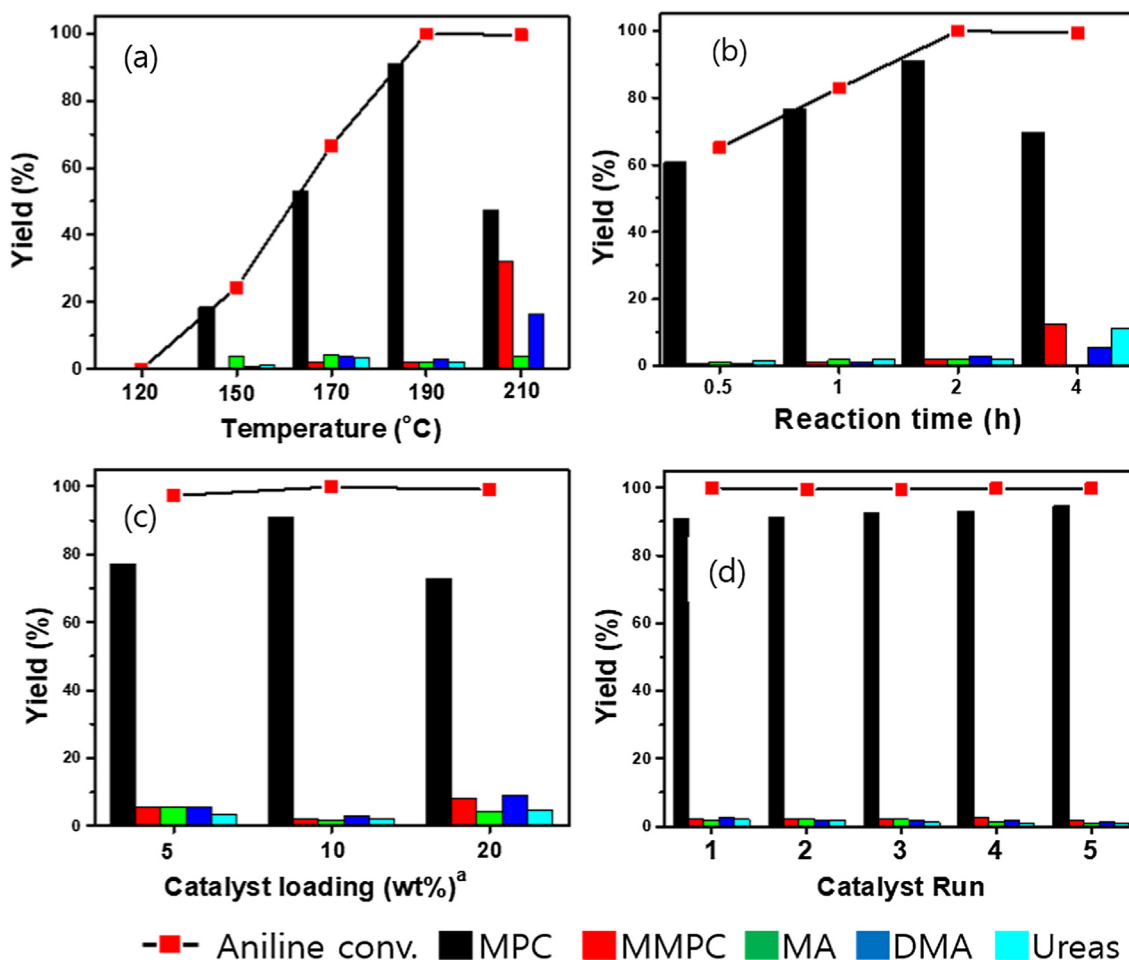


Fig. 11. Effect of (a) reaction temperature, (b) reaction time, (c) catalyst loading, and (d) catalyst reuse on the methoxycarbonylation of aniline with DMC reaction of ZIF-7-OAc treated DMC 6 h 190 °C. ^aCatalyst/aniline. Reaction condition: aniline 1.16 g, DMC 13.5 g, catalyst 0.116 g, 190 °C, 2 h.

ZIF-7 and water in the DMC, forming the species (I) depicted in Scheme 3 [30]. Then, the OH groups are turned into methoxycarbonyloxy groups by the reaction with DMC, species (II). At this step, according to the ¹H NMR analysis in Table 2, it seems some OH groups remain. The benzimidazole groups attached to the near Zn site could be replaced by DMC, species (III), which induces carbonyl group activation in DMC. The nucleophilic attack of aniline on the carbonyl group in DMC produces MPC, species (IV) and the produced MPC can be replaced by the abundant DMC for further methoxycarbonylation reactions.

4. Conclusion

Various versions of ZIF-7, Zn(BeIm)₂ were synthesized using the zinc precursors Zn(OAc)₂, ZnCl₂, ZnBr₂, Zn(NO₃)₂ and benzimidazole. The synthesized ZIF-7s showed similar catalytic activity for the methoxycarbonylation reaction of aniline, and dimethyl carbonate, irrespective of their surface area and morphologies. The yields of methyl phenyl carbamate (MPC) were 60–70% with >95% aniline conversion at 190 °C for 2 h reaction. The reusability study revealed that MPC yield increased with increasing catalyst reuse, and reached 94.7% after the 6th run, with suppressed methylation side products. The increase in catalytic activity of the ZIF-7 with increasing catalyst reuse could be ascribed to the formation of an active site from the defect sites or vacant sites made by leaching of the benzimidazole ligand from the zinc center. The DMC seemed to be activated by this catalyst site. Pretreatment

of ZIF-7 with DMC activated the catalyst directly and the best pretreatment condition was 190 °C for 6 h. The activated catalyst showed 91.0% MPC yield and the yield increased to 94.7% at the 4th reuse.

Acknowledgements

This work was supported by C1 Gas Refinery Program through the National Research Foundation of Korea (NRF) (NRF-2015M3D3A1A01065435) and KIST internal program (2E29500).

Appendix A. Supplementary material

Supplementary data to this article can be found online at <https://doi.org/10.1016/j.jcat.2019.09.039>.

References

- [1] P. Tundo, M. Musolino, F. Aricò, *Green Chem.* 20 (2018) 28–85.
- [2] P. Tundo, M. Selva, *Acc. Chem. Res.* 35 (2002) 706–716.
- [3] T. Baba, A. Kobayashi, Y. Kawanami, K. Inazu, A. Ishikawa, T. Echizen, K. Murai, S. Aso, M. Inomata, *Green Chem.* 7 (2005) 159–165.
- [4] E. Reixach, R.M. Haak, S. Wershofen, A. Vidal-Ferran, *Ind. Eng. Chem. Res.* 51 (2012) 16165–16170.
- [5] Z.-H. Fu, Y. Ono, *J. Mol. Catal.* 91 (1994) 399–405.
- [6] S. Wang, G. Zhang, X. Ma, J. Gong, *Ind. Eng. Chem. Res.* 46 (2007) 6858–6864.
- [7] M. Curini, F. Epifano, F. Maltese, O. Rosati, *Tetrahedron Lett.* 43 (2002) 4895–4897.
- [8] X. Zhao, Y. Wang, S. Wang, H. Yang, J. Zhang, *Ind. Eng. Chem. Res.* 41 (2002) 5139–5144.

- [9] F. Li, W. Li, J. Li, W. Xue, Y. Wang, X. Zhao, *Appl. Catal. A Gen.* 475 (2014) 355–362.
- [10] F. Li, Y. Wang, W. Xue, X. Zhao, *J. Chem. Technol. Biotechnol.* 84 (2009) 48–53.
- [11] F. Li, J. Miao, Y. Wang, X. Zhao, *Ind. Eng. Chem. Res.* 45 (2006) 4892–4897.
- [12] N. Lucas, A.P. Amrute, K. Palraj, G.V. Shanbhag, A. Vinu, S.B. Halligudi, *J. Mol. Catal. A Chem.* 295 (2008) 29–33.
- [13] X. Guo, Z. Qin, W. Fan, G. Wang, R. Zhao, S. Peng, *J. Wang, Catal. Lett.* 128 (2009) 405–412.
- [14] Y. Wang, B. Liu, *Catal. Sci. Technol.* 5 (2015) 109–113.
- [15] K.S. Park, Z. Ni, A.P. Côté, J.Y. Choi, R. Huang, F.J. Uribe-Romo, H.K. Chae, M. O’Keeffe, O.M. Yaghi, *Proc. Natl. Acad. Sci.* 103 (2006) 10186.
- [16] M. He, J. Yao, Q. Liu, K. Wang, F. Chen, H. Wang, *Microporous Mesoporous Mater.* 184 (2014) 55–60.
- [17] G. Lu, J.T. Hupp, *J. Am. Chem. Soc.* 132 (2010) 7832–7833.
- [18] M. Tu, S. Wannapaiboon, K. Khaletskaia, R.A. Fischer, *Adv. Funct. Mater.* 25 (2015) 4470–4479.
- [19] Y. Hwang, H. Sohn, A. Phan, O.M. Yaghi, R.N. Candler, *Nano Lett.* 13 (2013) 5271–5276.
- [20] D. Fairen-Jimenez, S.A. Moggach, M.T. Wharmby, P.A. Wright, S. Parsons, T. Düren, *J. Am. Chem. Soc.* 133 (2011) 8900–8902.
- [21] L. Li, J. Yao, R. Chen, L. He, K. Wang, H. Wang, *Microporous Mesoporous Mater.* 168 (2013) 15–18.
- [22] A. Huang, W. Dou, J. Caro, *J. Am. Chem. Soc.* 132 (2010) 15562–15564.
- [23] A. Arami-Niya, G. Birkett, Z. Zhu, T.E. Rufford, *J. Mater. Chem. A* 5 (2017) 21389–21399.
- [24] C. Gücüyener, J. van den Bergh, J. Gascon, F. Kapteijn, *J. Am. Chem. Soc.* 132 (2010) 17704–17706.
- [25] L.T.L. Nguyen, K.K.A. Le, H.X. Truong, N.T.S. Phan, *Catal. Sci. Technol.* 2 (2012) 521–528.
- [26] J. Kim, S.-N. Kim, H.-G. Jang, G. Seo, W.-S. Ahn, *Appl. Catal. A Gen.* 453 (2013) 175–180.
- [27] C.M. Miralda, E.E. Macias, M. Zhu, P. Ratnasamy, M.A. Carreon, *ACS Catal.* 2 (2012) 180–183.
- [28] A. Zhang, L. Li, J. Li, Y. Zhang, S. Gao, *Catal. Commun.* 12 (2011) 1183–1187.
- [29] L.H. Wee, T. Lescouet, J. Ethiraj, F. Bonino, R. Vidruk, E. Garrier, D. Packet, S. Bordiga, D. Farrusseng, M. Herskowitz, J.A. Martens, *ChemCatChem* 5 (2013) 3562–3566.
- [30] C. Chizallet, S. Lazare, D. Bazer-Bachi, F. Bonnier, V. Lecocq, E. Soyer, A.-A. Quoineaud, N. Bats, *J. Am. Chem. Soc.* 132 (2010) 12365–12377.
- [31] P. Zhao, G.I. Lampronti, G.O. Lloyd, E. Suard, S.A.T. Redfern, *J. Mater. Chem. A* 2 (2014) 620–623.
- [32] Y. Du, B. Wooller, M. Nines, P. Kortunov, C.S. Paur, J. Zengel, S.C. Weston, P.I. Ravikovitch, *J. Am. Chem. Soc.* 137 (2015) 13603–13611.
- [33] P. Valvekens, F. Vermoortele, D. De Vos, *Catal. Sci. Technol.* 3 (2013) 1435–1445.
- [34] F. Vermoortele, B. Bueken, G. Le Bars, B. Van de Voorde, M. Vandichel, K. Houthoofd, A. Vimont, M. Daturi, M. Waroquier, V. Van Speybroeck, C. Kirschhock, D.E. De Vos, *J. Am. Chem. Soc.* 135 (2013) 11465–11468.
- [35] F. Tian, A.M. Cerro, A.M. Mosier, H.K. Wayment-Steele, R.S. Shine, A. Park, E.R. Webster, L.E. Johnson, M.S. Johal, L. Benz, *J. Phys. Chem. C* 118 (2014) 14449–14456.
- [36] M.J. Lee, H.T. Kwon, H.-K. Jeong, *J. Membr. Sci.* 529 (2017) 105–113.
- [37] W. Cai, T. Lee, M. Lee, W. Cho, D.-Y. Han, N. Choi, A.C.K. Yip, J. Choi, *J. Am. Chem. Soc.* 136 (2014) 7961–7971.
- [38] S. Grego, F. Arico, P. Tundo, *Pure Appl. Chem.* 84 (2012) 695–705.
- [39] S. Aguado, G. Bergeret, M.P. Titus, V. Moizan, C. Nieto-Draghi, N. Bats, D. Farrusseng, *New J. Chem.* 35 (2011) 546–550.
- [40] M. He, J. Yao, L. Li, K. Wang, F. Chen, H. Wang, *Chempluschem* 78 (2013) 1222–1225.
- [41] C. Zhang, C. Han, D.S. Sholl, J.R. Schmidt, *J. Phys. Chem. Lett.* 7 (2016) 459–464.
- [42] M. Takahashi, H. Tanida, S. Kawauchi, M. Harada, I. Watanabe, *J. Synchrotron Radiat.* 6 (1999) 278–280.
- [43] S.J. Borg, W. Liu, *Nucl. Instrum. Methods Phys. Res. Sect. A Accel. Spectrom. Detect. Assoc. Equip.* 619 (2010) 276–279.
- [44] M. Goesten, E. Stavitski, E.A. Pidko, C. Gücüyener, B. Boshuizen, S.N. Ehrlich, E.J. M. Hensen, F. Kapteijn, *J. Gascon, Chem. – A Eur. J.* 19 (2013) 7809–7816, <https://doi.org/10.1002/chem.201204638>.